Microwave Instrumentation for Radio Astronomy

John C. Webber and Marian W. Pospieszalski, *Fellow, IEEE*

Invited Paper

***Abstract*—Radio astronomy is a branch of science that allows observation of natural radio signals from cosmic sources. Microwave techniques are employed in large radio telescope systems in diverse ways. Starting with early vacuum tube receivers at meter wavelengths, low-noise receivers have pushed the leading edge of technology, culminating in present-day receivers employing HFET amplifiers, superconducting tunnel junctions, and other advanced receiving elements. We discuss the principles of such devices, modern receivers, and modern radio telescope systems both operational and under development.**

***Index Terms*—Amplifiers, radio astronomy, radio receivers, superconductor–insulator–superconductor mixers.**

I. Introduction

RADIO astronomy as a branch of science was born in 1932 with the discovery by Jansky of "electrical disturbances apparently of extra terrestrial origin" [1]. As a branch of science it encompasses many topics: astronomy, physics, chemistry, and many fields of engineering. Kraus, in the preface to his book [2], which was the first comprehensive treatment of the field, wrote "radio astronomy embraces a wide range of topics from physical phenomena to receiver and antenna design." This paper, therefore, can give only a glimpse of this broad and fascinating field; it is intended to explore the connection of radio astronomy to the field of interest of the IEEE Microwave Theory and Techniques Society (IEEE MTT-S).

New developments in microwave technology have made possible the creation of more complex and sensitive instruments, which, over the last 50 years, have brought about fascinating discoveries about our solar system, other solar systems, the interstellar medium, galaxies, and the evolution of the Universe. Jansky's discovery of "a steady hiss type static of unknown origin" was discovered at a wavelength of 14.6 m, hardly what one would classify as microwaves today. Soon the experiments shifted to much higher frequencies with early attempts by Reber in 1937 to observe at 10- and 33-cm wavelengths and his successful observations of the galactic plane at 187-cm wavelength [3]. Progress in microwave technology during and after World War II allowed for great advances in radio astronomy antenna and receiver technologies. These advances brought about a steady stream of important discoveries. These include the discovery of radiation from the Sun and Moon (1946), the discovery of radiation from galactic hydrogen (1951), radio observations of the OH lines in the interstellar medium (1963) followed by discovery of many other lines of interstellar species, the discovery of quasars (1963), the discovery of the cosmic microwave background radiation (CMBR) (1965), and the discovery of pulsars (1967). One could add at the end of this very incomplete list the relatively recent discoveries of radio evidence for the existence of black holes, gravitational wave radiation, details of the birth of stars and other solar systems, and the discovery of the anisotropy of the CMBR, which directly measures the structure of the early Universe. An excellent summary of pre-1988 research and development is contained in [4].

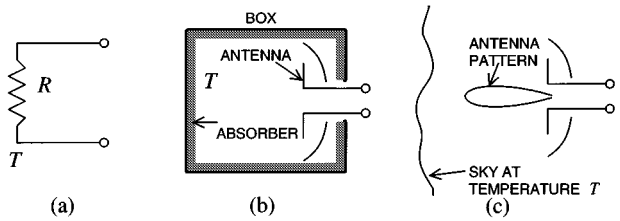

Fig. 1. (a) Resistor at temperature T. (b) Antenna in an absorbing box at temperature T. (c) Antenna observing sky at temperature T (after [2]).

This paper is intended to introduce the reader to the basic concepts used in radio astronomy and provide a short review of microwave instrumentation used in this field. In Section II, the basic radiometric and interferometric concepts are introduced. Section III provides a review of low-noise devices used in radio astronomy receivers, while Section IV gives examples of radio astronomy receivers. A glimpse of existing radio astronomy observatories, and a short review of current and future projects are given in Sections V and VI.

II. Fundamental Principles

A. Radiometers

Consider the situation shown schematically in Fig. 1 (after [2]). The available noise power in a unit bandwidth p of a resistor [see Fig. 1(a)] at a certain temperature T is given by the Nyquist relation, which under the Rayleigh-Jeans approximation to the Planck law is

$$p = kT \tag{1}$$

where $k = 1.38 \times 10^{-23}$ J K^{-1} (Boltzmann constant) and T is the absolute temperature. The resistance of that resistor can

Manuscript received October 22, 2001.

The authors are with the National Radio Astronomy Observatory, Charlottesville, VA 22901 USA (e-mail: jwebber@nrao.edu; mpospies@nrao.edu).

Publisher Item Identifier S 0018-9480(02)01957-9.

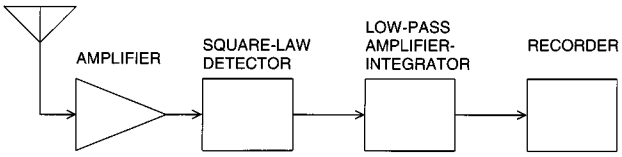

Fig. 2. Simplified block diagram of a total power receiver.

be chosen to be exactly that of the radiation resistance of an ideal lossless antenna whose radiation pattern is completely enclosed by a black body also at temperature T [see Fig. 1(b)]. In this case, the power available at the antenna terminals under the Rayleigh–Jeans approximation to the Planck black-body radiation law is [2]

$$p = \frac{kT}{\lambda^2} A_e \Omega_A \tag{2}$$

where λ is the wavelength, A_e is the effective aperture of the antenna, and Ω_A is the solid angle of the beam of the antenna. It is known from antenna theory that

$$A_e \Omega_A = \lambda^2. \tag{3}$$

Upon substitution of (3) into (2), (1) is obtained, i.e., the available noise power at the ideal antenna terminals of Fig. 2 is exactly the same as that of a resistor. In the third case, shown in Fig. 1(c), the sky having a certain temperature T completely fills the solid angle of the antenna pattern. In this case, the available power at the antenna terminals is exactly the same as in previous two cases. In general, the effective temperature of the antenna radiation resistance is called antenna temperature T_A.

For a radio source with a given brightness distribution $B(\theta, \phi)$, the integral of the brightness of the source yields the total source flux density

$$p = kT_A = \frac{1}{2} A_e \iint B(\theta, \phi) P_n(\theta, \phi) d\Omega \tag{4}$$

where $P_n(\theta, \phi)$ is the antenna radiation pattern. Assuming that the angular size of the source is much smaller than the antenna solid angle (the source is not resolved), the total flux density S_o of the radio source is given [2] by

$$S_o = \frac{2kT_A}{A_e}. \tag{5}$$

Assume now that a receiver is connected to the antenna terminals. The noise temperature T_R of such a receiver (under the Rayleigh–Jeans or Planck formulations) is defined as the noise temperature of a resistor, which connected to the input of a noiseless, but otherwise identical receiver, gives the same output noise power density as that of the actual receiver connected to a resistor source of absolute zero temperature (for an in-depth discussion of the validity of this definition when zero point noise is taken into account, see [43]). Consequently, the noise power at the output of a receiver connected to the antenna is proportional to the sum of antenna temperature T_A and receiver temperature T_R, which is usually called the system noise temperature T_S.

In a basic radio astronomy system, the noise-like signal proportional to the system temperature after sufficient amplification in a given bandwidth B is detected by a square law detector, and then integrated for a time t. Such a radio astronomy receiver is known as a total power radiometer (Fig. 2). In this ideal case, the radiometer sensitivity, or minimum detectable temperature ΔT of a radio telescope is equal to the rms variation of the detected and integrated signal. This can be shown to be given by [2]

$$\Delta T = T_S \frac{1}{\sqrt{Bt}}. \tag{6}$$

Consequently, the minimum detectable flux density ΔS from the radio source is given by

$$\Delta S = \frac{2k}{A_e} \Delta T. \tag{7}$$

In principle, the minimum detectable temperature can be made arbitrarily small, given sufficiently long integration time. For a ground-based telescope looking at the celestial pole, the minimum possible antenna temperature is limited by two factors: the radiation of the atmosphere, typically a few kelvin at microwave frequencies at a high dry site; and the CMBR temperature, which is equal to 2.725 K. To these must be added the effects of spillover and ohmic losses in the antenna and feed structures—typically a few more kelvin. This underscores the importance of equipping radio telescopes with receivers having extremely low noise temperatures. For detection of faint radio sources, the telescope should have as large an effective aperture as possible. In contrast, a space-based radiometer looking at the Earth will always see an antenna temperature close to 300 K.

The equation for the minimum detectable temperature is derived under the assumption that the total receiver predetection gain does not change over the integration time. If this effect of random changes of the receiver gain is taken into account, the sensitivity of the total power receiver can be stated as [2]

$$\Delta T = T_S \sqrt{\frac{1}{Bt} + \left(\frac{\Delta G}{G}\right)^2} \tag{8}$$

where G is predetection average gain and ΔG is the effective value of power gain variations. The gain changes can be due to the elements external to the receiver (temperature, bias, *etc.*), which, to a large degree, can be controlled. More importantly, all amplifying elements exhibit random gain fluctuation, typically inversely proportional to frequency, which may limit the performance of modern radiometers having many gigahertz of instantaneous bandwidth.

The effect of gain variations may be alleviated by using a so-called switched or Dicke receiver or a correlation receiver; there are many variations of these two principal schemes. The first uses the principle of comparing the received signal with a reference load on a time scale much shorter than that of the gain variations. The correlation receiver uses two independent amplifying chains whose outputs are multiplied and averaged and will, therefore, produce no dc signal due to random gain fluctuations, as these are statistically independent in the two amplifying chains. For the details of different schemes, the reader is referred to [2] and [34].

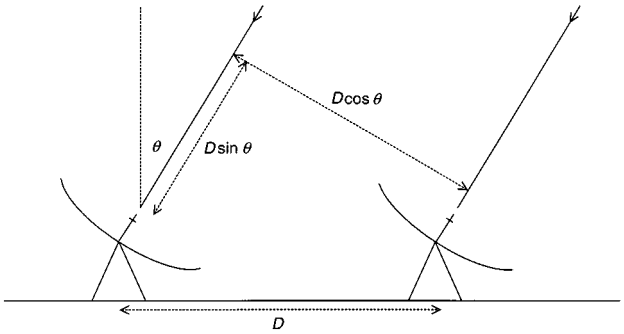

Fig. 3. Geometry of a simple two-element interferometer.

B. Interferometers

While large single antennas are extensively employed, much higher angular resolution without the need to build antennas of impractical size may be obtained by building interferometers. The angular resolution of an interferometer is of the order of λ/D, where D is the maximum separation of any two elements [6]. Each element of such an interferometer is a single antenna, usually identical to all the others. Coherent local oscillator (LO) signals are provided at each element, usually through direct distribution. In the case of very long baseline interferometry (VLBI), in which antennas may be on different continents or even in space [5], this is accomplished by installing sufficiently stable independent oscillators and recording the received signals for playback and cross-multiplication (correlation) at a central site.

In the elementary interferometer shown in Fig. 3 (after [6]), two antennas separated by distance D in the East–West direction are pointed at the same celestial source, at an angle θ from the zenith. Note that the signal arrives at the right-hand antenna first, and that, as the Earth rotates, angle θ changes, so that the projected baseline $D\cos\theta$ and the signal propagation differential distance $D\sin\theta$ change as well. This makes a narrow-band signal received by both antennas go in and out of phase periodically. If the two signals are simply multiplied, it can be shown that the output F of the multiplier, or *fringe function*, is given by

$$F = \cos\left(\frac{2\pi D\sin\theta}{\lambda}\right). \tag{9}$$

If there are multiple antennas, then the products of all pairs of antennas may be obtained. The results are set of so-called *visibilities*, each of which constitutes a measurement of the amplitude and phase of the signals from a pair of antennas at a particular time. If a radio source is tracked by all elements of the interferometer over a period of time, providing visibilities over a wide range of angles, then it is possible from a two-dimensional Fourier transform of the visibility data to determine the structure of the source, *i.e.*, to make an image or radio picture. This is known as *aperture synthesis*, for which Sir Martin Ryle was awarded the Nobel Prize in physics in 1974. This technique is the subject of a very extensive body of work, beyond the scope of this paper, and the reader is referred to [6] for a comprehensive treatment of all aspects of radio interferometry.

In addition to making images, it is possible to use interferometry to determine with great accuracy the relative positions of the interferometer elements. This is done by measuring many radio sources, of small diameter so that they are unresolved by the interferometer, over a wide range of observing angles. It is possible with VLBI techniques to measure the relative locations of elements separated by thousands of kilometers to an accuracy of a few millimeters. This technique has been extensively employed to measure the continental drift of the Earth's tectonic plates [7].

III. Low-Noise Devices

A. General Remarks

The quest for ultra-low-noise reception is especially important for radio astronomy, as the receiver noise is usually a significant part of the system noise. A list of devices, which at one time provided the lowest reported noise temperature in some frequency band, is very long: vacuum tubes, crystal mixers, tunnel diode amplifiers, parametric amplifiers, solid-state masers, Schottky diode mixers, superconductor–insulator–superconductor (SIS) mixers, GaAs field-effect transistors (FETs) and heterostructure field-effect transistors (HFETs), hot electron bolometers (HEBs), etc. Okwit gives a very interesting historical review of the pre 1970s evolution of low-noise concepts and techniques [8]. Relevant information concerning developments in the 1960s and 1970s can also be found in two Special Issues of this TRANSACTIONS ("Special Issue on Noise," Sept. 1968; "Special Issue on Low Noise Technology," Apr. 1977).

Three of the low-noise devices mentioned above, namely solid-state masers, SIS mixers, and HEBs, will operate only at cryogenic temperatures. Most other devices (with the exception of vacuum tubes) have also been cooled to cryogenic temperatures for two main reasons: improvement in the device performance, usually due to the improvement of the electron transport properties, and reduction of the influence of thermal noise generated by parasitic elements [9]–[11].

In the early 1970s, the ultra-low-noise receiving systems employed mainly solid-state masers, cryogenically cooled parametric amplifiers (or converters), and Schottky diode mixers. At the end of that decade, the advances in the technology of GaAs FETs, combined with cryogenic cooling, made the noise performance of GaAs FET amplifiers competitive with the performance of parametric amplifiers [10]. Also, a new mixing element, the SIS tunnel junction capable of almost quantum limited detection, was developed [12]–[15]. In modern radio astronomy instrumentation, HFET receivers now compete in performance with masers and SIS/HFET mixer–preamplifiers for frequencies below approximately 120 GHz. At frequencies above 120 GHz and up to approximately 1 THz, SIS mixers demonstrate the best noise performance. Above 1 THz, cooled Schottky diode mixers and HEB mixers provide the lowest noise temperatures. Ruby masers are still sometimes used in Deep Space Network antennas at X- and Ka-band frequencies [16].

B. HFET Amplifiers

Progress in the noise performance of FET and HFET amplifiers at cryogenic temperatures in the last quarter century was quite dramatic. In 1980, a noise temperature of 20 K at a fre-

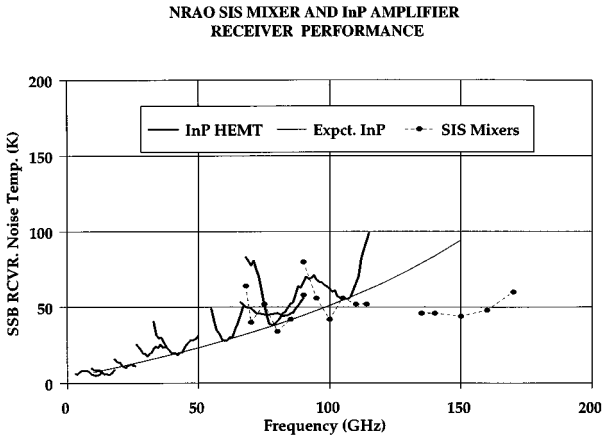

Fig. 4. Comparison of noise temperature of NRAO cryogenic receivers using InP HFET amplifiers cooled to approximately 20 K and SIS mixer receivers cooled to 4 K.

quency of 4.75 GHz was measured at a physical temperature of 18 K for a GaAs FET having 0.7-μm-long gate [10]. In 1993, under similar conditions, a noise temperature of 15 K was measured at a frequency of 43 GHz [17] for an InP lattice-matched heterostructure FET having a 0.1-μm-long gate. This progress has been achieved by addressing the following two issues in FET (HFET) design: 1) maximization of intrinsic cutoff frequency $f_T = g_m/2\pi C_{gs}$, where g_m and C_{gs} are the transconductance and gate capacitance, respectively, and 2) minimization of parasitic resistances of gate and source r_g and r_s, respectively.

Since 1993, progress in noise performance of HFETs has not been significant. However, the technology of InP devices has matured and allowed practical use. Hybrid "chip and wire" amplifiers have been demonstrated up to frequencies of 118 GHz and successfully used in several instruments for radio astronomy research [21], [28], [31]. These include the very large array (VLA), the very long baseline array (VLBA), the Green Bank telescope (GBT), the microwave anisotropy probe (MAP), and several ground-based instruments for the investigation of the cosmic microwave background. A number of monolithic microwave integrated circuit (MMIC) designs were demonstrated at room temperature up to 190 GHz [18], [19] and up to 115 GHz for cryogenic applications [20].

A summary of the noise performance of laboratory receivers using HFET amplifiers cooled to approximately 20 K and a comparison with the typical performance of SIS mixer receivers cooled to 4 K is presented in Fig. 4. Fig. 4 also shows the best performance of InP HFET receivers expected at any frequency for current state-of-the-art devices. This graph is based on the minimum noise measure of a state-of-the-art 0.1-μm gatelength InP HFET. The minimum noise measure is equal to the minimum noise temperature of an amplifier with an infinite number of stages, each stage with an optimal embedding circuit. Therefore, it establishes a limit of noise performance of a receiver in which an amplifier has sufficient gain to make the contribution of subsequent mixer and/or amplifiers insignificant. A broad-band HFET amplifier design [21], [32] can attain the noise temperature equal to the minimum noise measure only at discrete frequencies, a property clearly illustrated in Fig. 4. Also, the examples in Fig. 4 demonstrate that, for a typical rectangular waveguide band, the average noise temperature is approximately equal to the value determined by the minimum noise measure at the highest frequency within the band. Fig. 5 shows examples of noise and gain performance of wide-band 3–13 and 8–18-GHz amplifiers, each having a total power dissipation of about 7 mW. An example of the noise performance of a wide-band laboratory receiver covering 68–118 GHz is shown in Fig. 6. The amplifier has gain $>$30 dB and uses about 30 mW of power.

C. SIS Mixers

An SIS mixer employs a superconducting tunnel junction as the nonlinear mixing element. These devices exhibit ac and dc Josephson tunneling currents (Cooper-pair currents), and also a single-electron (quasi-particle) tunneling current. It is the strong nonlinearity of the quasi-particle current versus voltage characteristic that is used in an SIS mixer; the Josephson currents can interfere with the mixing process and are often suppressed by application of a magnetic field. While SIS mixers are *resistive* mixers (as are Schottky diode mixers), their strong nonlinearity results in nonclassical (quantum) effects—possible gain and negative resistance—and their analysis and design are quite complex; a comprehensive review of theory and design principles is given in [23]. A high-quality SIS mixer can have a noise temperature $\sim hf/k$ ($\sim$5 K at 100 GHz), and is typically followed by an IF amplifier, which may contribute a significant portion of the receiver noise. The upper useful frequency of an SIS mixer is limited by the energy gap of the superconductor. For niobium junctions, this limit is $\sim$700 GHz.

SIS mixers were first reported in 1979 [12], [13]. Early SIS mixers employed Pb-alloy junctions, which required cooling to 2.5-K temperature for satisfactory operation. These junctions were very sensitive to moisture and electrical shock and required special moisture-free and/or cryogenic storage. Modern SIS mixers normally use Nb junctions, which give good results when cooled to 4.0-K physical temperature, which is conveniently reached with boiling He. Junction sizes are typically a few square micrometers, and critical current densities are typically a few thousand A/cm^2. Most designs to date have employed an IF bandwidth of $\leq$1 GHz, with the exception of an approximately 3-GHz bandwidth reported in [24]. Using an SIS mixer designed for low-output capacitance [26], an IF bandwidth of 8 GHz (4–12 GHz) has recently been achieved [25]. Obtaining such wide IF bandwidth requires that the IF amplifier be integrated closely with the mixer, forming an inseparable mixer–preamplifier module.

Most early SIS mixers had adjustable RF tuning elements in order to cover the desired frequency range [44]. More recently, tunerless designs have achieved waveguide-band frequency coverage [26], [39], [40] and eliminated the need for moving parts within the cryostat, a great advantage in terms of cost and reliability. The performance of a representative SIS mixer for 200–290 GHz is shown in Fig. 7.

In order to achieve the sensitivity advantage of single-sideband operation, MMIC SIS sideband-separating mixers have

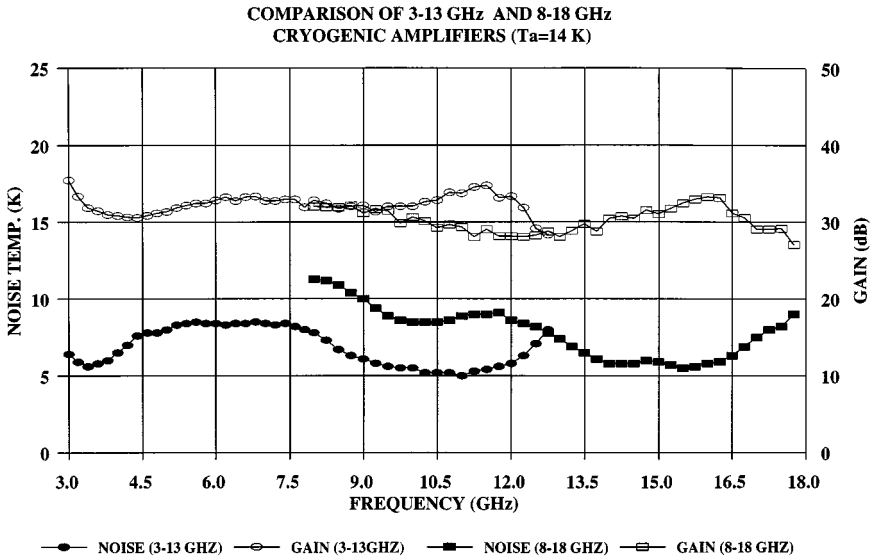

Fig. 5. Example of cryogenic performance of 3–13- and 8–18-GHz amplifiers using InP HFETs. For each amplifier, the total power dissipation is 7 mW.

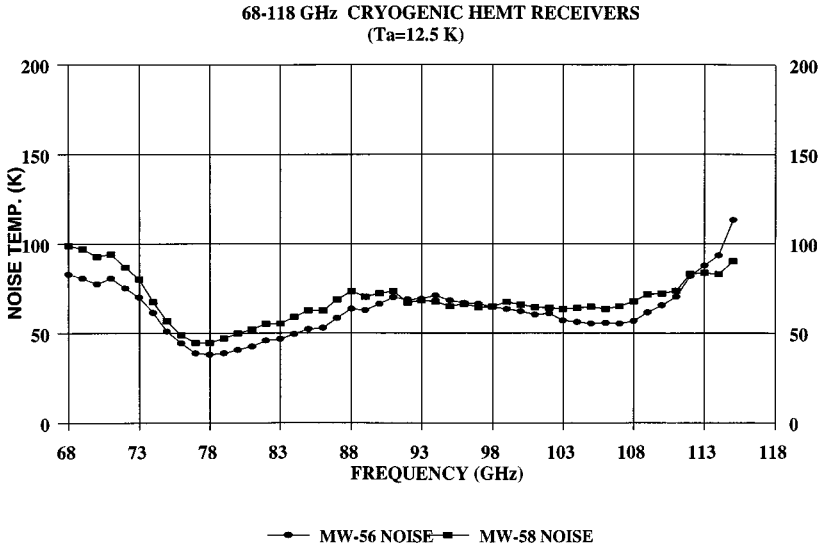

Fig. 6. Examples of noise performance of a 68–118-GHz InP HFET receiver using two different amplifiers, serial numbers MW-56 and MW-58.

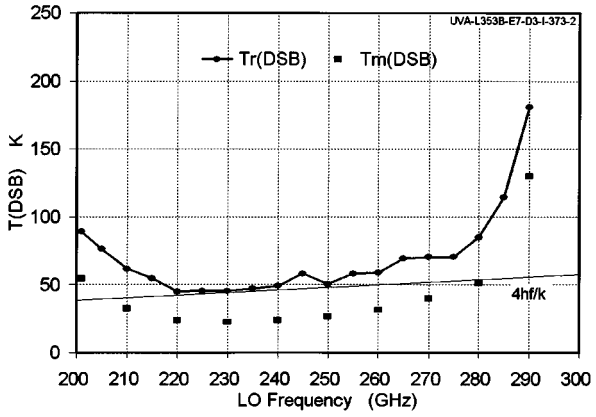

Fig. 7. Example of noise performance of a fixed-tuned SIS mixer (discrete points) and the entire receiver (solid line) for 200–290 GHz.

been developed that include quadrature hybrids, LO couplers, and a cold image termination on a single small quartz chip [27], [42][1]. In addition, a balanced SIS mixer has the same advantages as a balanced conventional mixer: reduction of the required LO power and canceling of the LO sideband noise downconverted into the IF band. A balanced SIS mixer using niobium MMIC technology has been demonstrated at 200–300 GHz [41][2], [42]. For ALMA (see Section VI), the goal for some of the bands is to have tunerless balanced sideband-separating operation with integrated wide-bandwidth preamplifiers [28].

IV. Examples of Radio Astronomy Receivers

A. HFET Receiver

The general concept of a compact low-noise HFET receiver for radio astronomy applications has been outlined by Weinreb

[1]Reference [42] is available online as ALMA Memo 151. [Online]. Available: http://www.mma.nrao.edu/memos/html-memos/abstracts

[2]Reference [41] is available online as ALMA Memo 308. [Online]. Available: http://www.mma.nrao.edu/memos/html-memos/abstracts

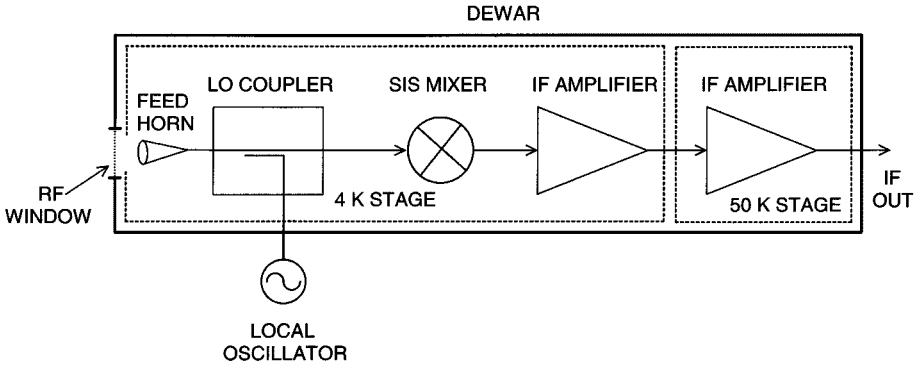

Fig. 8. Simplified block diagram of an SIS mixer receiver.

et al. [29] and several examples are given therein. A critical area in very low-noise receiver design is a low-loss coupling between an ambient temperature feed horn and a cryogenic amplifier. The VLBA front-ends [30] use a gapped circular waveguide transition from the feed to a cooled polarizer located within the vacuum Dewar. Noise calibration signals are injected through cooled directional couplers. A careful thermal design allows all of these components to be cooled by a small closed-cycle refrigerator to approximately 13 K. There can be significant noise degradation due to the cumulative losses of vacuum window, horn, polarizer, coupler, isolator, and connecting components. This is why, in modern receivers, all those components are cooled together with an amplifier unless their sizes make it impractical to do so. For cases in which all the components are cooled, the noise temperature of a state-of-the-art receiver will be as presented in Fig. 4.

In reference to the discussion in Section II, a state-of-the-art 8-GHz receiver can exhibit noise temperature T_R of less than 10 K, while the antenna temperature of the VLBA antenna at this frequency T_A would typically be approximately 20 K, for a total system noise of approximately 30 K. Therefore, the noise of a low-noise device (about 4 K at this frequency) is no longer a dominant factor determining the system noise temperature of some telescopes. For new antennas, a careful analysis of the influence of sidelobe levels, spillover characteristics, efficiency, etc. on system noise temperature is required. For example, the GBT [31] had all these parameters carefully optimized; the antenna temperature T_A for frequencies between 1–10 GHz is expected to be less than 10 K.

B. SIS Receiver

SIS mixer receivers are typically employed above frequencies of about 100 GHz since they exhibit lower noise than HFET amplifiers in this domain. The problems of coupling the radiation into the mixer are the same as for HFET receivers, made even more difficult by smaller dimensions and tolerances as the frequency is increased. Double-sideband receiver noise temperatures of approximately 20 K have been reported near 100 GHz for Nb SIS mixer receivers, with an increase in noise roughly proportional to frequency up to the bandgap frequency of 700 GHz. An SIS receiver has some advantages over an HFET receiver in that a single conversion is performed to the adopted baseband. HFET amplifiers require an additional conventional mixer, and are intrinsically single sideband; in order to achieve wide tunable bandwidth, it may be necessary to employ two IF stages in order to preserve single-sideband operation, adding to the complexity and cost of the receiver. On the other hand, HFET amplifiers give satisfactory operation at a physical temperature of 20 K, which is easier and more economical than 4-K operation. A simplified block diagram of a conventional SIS mixer receiver is shown in Fig. 8.

To date, most SIS mixer receivers have been operated in a double-sideband configuration, which degrades the signal-to-noise ratio achievable in spectroscopic observations. In some receivers, the unwanted sideband is canceled by interferometric techniques; however, this method can be employed only over a limited bandwidth. Single-sideband SIS mixer operation over a wide bandwidth can be achieved with a sideband-separating mixer such as has been previously described. In this case, the achievable image rejection of roughly 20 dB is not as good as that of an HFET amplifier receiver, but it is quite adequate for most applications.

C. MAP Radiometer

The HFET or SIS receivers discussed in Sections IV-A and B are typically used in conjunction with a back-end signal-processing system, which allows observations with user-selectable frequency resolution. This is important for spectroscopic or “line” observing, in which observation of the emission or absorption of radiation at a particular frequency due to an atomic or molecular species is the goal. On the other hand, if the observed radiation is of thermal origin (or otherwise possesses a spectrum slowly varying in frequency), then the largest possible radiometer bandwidth allows for greater sensitivity (Section II). Modern instruments are, therefore, constructed in such a way that they can deliver to the detector the largest practical bandwidth. In modern radio telescopes, this typically varies from approximately 0.5 to 8 GHz. Some dedicated instruments, however, especially those investigating the Cosmic Microwave Background, do not use frequency conversion but detect directly the wide-band RF power after it is sufficiently amplified. Modern examples of such an approach are radiometers constructed for the MAP [32]–[34]. The MAP satellite was launched in June 2001 to make a full sky map of the CMBR with 20-μK sensitivity per $0.3^\circ \times 0.3^\circ$ pixel during the two-year lifetime of the mission. Differential pseu-

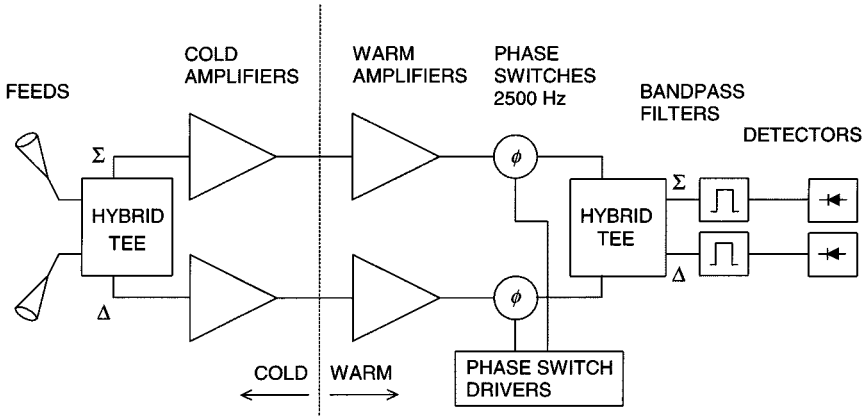

Fig. 9. Simplified block diagram of a MAP satellite pseudocorrelation radiometer.

docorrelation radiometers covering 20–25 GHz, 28–37 GHz, 35–46 GHz, 53–69 Hz, and 82–106 GHz are used in this mission [33], [34]. A schematic view of the MAP radiometer is shown in Fig. 9. It is similar in its function to a true correlation radiometer, which could not be implemented because multipliers with instantaneous bandwidth as wide as 20 GHz are not yet available. MAP radiometers measure the difference between the apparent temperatures of two points on the sky by first combining two sky signals in a hybrid tee (Fig. 9), then amplifying each combined signal in cold HFET amplifiers (to reduce noise) and then sending the phase-matched outputs to the warm amplifiers. At this point, one arm is phase switched between 0°–180°. The signals are recombined in a second hybrid tee. After filtering in identical wide-band filters, the signals are square-law detected and then undergo synchronous demodulation. Due to symmetry of design and careful matching of the complex gains of the two amplifier chains, random gain fluctuations of the amplifiers produce the same signals at both detectors and, thus, cancel when the detector outputs are differenced. Phase switching further allows removal of effects caused by detector gain variations [34].

Such an approach allows for a construction of an instrument whose outputs are stable on time scales of minutes, i.e., on these time scales, the sensitivity is determined by the system noise, effective bandwidth, and integration time. This stability is further enhanced by additional Dicke switching, which is simply obtained by rotation and precession of the spacecraft [33].

V. Examples of Radio Astronomy Observatories

Large single-dish antennas and interferometers with only a few elements were the workhorses of radio astronomy up to about 1980. These were employed both for full-sky surveys at various frequencies, just to determine what radio sources existed and where they were, and for extensive and detailed observations of individual sources. It is impossible here to list all the important facilities and their results. Particularly notable, however, were the 159- and 178-MHz (3C and 4C) radio surveys carried out by interferometers in Cambridge, U.K.; the 100-m-diameter steerable antenna at Effelsberg, Germany; the 140-foot-diameter antenna at Green Bank, WV; the WSRT interferometer at Westerbork, The Netherlands; the 64-m antennas at Parkes, Australia; and the 300-m-diameter antenna at Arecibo, Puerto Rico.

Fig. 10. Inner portion of the VLA in its most compact configuration.

A major addition to the world's radio observing facilities was made in 1980 with the commissioning of the VLA (Fig. 10) near Socorro, New Mexico, by the National Radio Astronomy Observatory (NRAO). This interferometer consists of 27 antennas, each of 25-m aperture, which are transportable on railroad tracks so that they may be configured either for short or long spacings, up to 36 km. The receiving bands extend from 74 MHz to 50 GHz, with incomplete frequency coverage. The angular resolution at the highest frequency and longest spacing is 0.05 arcseconds, so that radio images may be made with a resolution comparable to that of the Hubble Space Telescope. For 20 years, this instrument has been the major ground-based radio telescope in the world.

New single dish and interferometric radio observatories have been built and commissioned over the last 20 years; again, a comprehensive list is impossible. Particularly notable, however, are the very long baseline array of the NRAO, with antennas across the U.S., including Hawaii and St. Croix; the Berkeley–Illinois–Maryland array of millimeter antennas at Hat Creek, CA; the California Institute of Technogy (CalTech) array of millimeter antennas at the Owens Valley Radio Observatory near Bishop, CA; the Australia telescope arrays; and the 100-m-offset paraboloid antenna in Green Bank, WV, dedicated

Fig. 11. 100-meter Robert C. Byrd GBT.

in 2000 (Fig. 11). The latter antenna is of unique design, and incorporates 2004 adjustable antenna panels, which, when coupled with a laser ranging system, will permit accurate adjustment of the surface to compensate for gravitational, thermal, and wind effects.

VI. Future Projects

There are several radio observatory projects in the planning, development, or construction phases.

The sub-millimeter array (SMA) of the Smithsonian Astrophysical Observatory and Academia Sinica Institute of Astronomy and Astrophysics of Taiwan is an array of eight antennas of 6-m diameter, which will operate from frequencies of approximately 170 to 900 GHz [35]. This instrument is under construction, and several antennas have been installed and tested at the site on Mauna Kea, Hawaii.

The VLA in 2000 was provided with a doubling of angular resolution by incorporating the nearest VLBA antenna (at Pie Town, New Mexico) via a dedicated fiber-optic link. Also, starting in 1998, installation of new receivers for the 22-GHz band began; these incorporate much better low-noise amplifiers and feed-to-amplifier coupling than the old 1970s vintage receivers, and achieve a system temperature at the zenith of less than 50 K. These improvements are the first step in converting the VLA to the enhanced VLA (EVLA). Complete frequency coverage from 1 to 50 GHz with modern receivers will be installed, with possible addition of the 300–1000-MHz band. The existing waveguide-based data transmission system, with a usable bandwidth of 140 MHz, will be replaced with a fiber-optic-based system, providing up to 16 GHz of bandwidth. The correlator, which cross-multiplies the signals from all antenna pairs, will be replaced with a modern correlator, supplied by the Herzberg Institute of Astrophysics, Victoria, BC, Canada; the Universidad Nacional Autónoma de México is also a collaborator. There is a planned addition of approximately eight new antennas at spacings intermediate between that of the VLA and VLBA; thus, complete and accurate imaging of radio sources can be performed on all angular scales, constrained only by the diameter of the Earth.

The Atacama large millimeter array (ALMA) is an international project among the U.S., Canada, several European nations and organizations, and Japan to build an array of 64 12-m-diameter antennas to operate from 31 to 900 GHz. It is a planned to be a merger of three projects, i.e., the U.S. MMA [36], the European LSA [37], and the Japanese LMSA [38]. This array is to be installed at an altitude of 5000 m in the northern desert of Chile, near the town of San Pedro de Atacama. It will provide resolution and sensitivity for millimeter and submillimeter wavelengths comparable to that of the VLA at centimeter wavelengths. This project is currently funded for construction, with completion targeted for 2010.

The Allen telescope array (ATA) is planned as an array of 350 6-m-diameter antennas, having the effective collecting area of a 100-m single dish, and operating over the frequency band of 0.5–11 GHz. The antennas will be connected to a central site by optical fiber. The signal processing will permit synthesis of multiple simultaneous narrow beams within the rather wide primary beam of the small antennas. Each such synthesized beam can be pointed to a different radio source, or in the case of search for extraterrestrial intelligence (SETI) a different star. This is a joint project of the University of California at Berkeley and the SETI institute. It is currently in a design and development phase, and is planned for completion in 2008.

A very large low-frequency array (LOFAR) is planned for the frequency range of 10–240 MHz. It will have a collecting area of 1 km^2 at a frequency of 15 MHz. For the long wavelengths involved, arrays of dipoles or patch antennas are a better choice than parabolic dishes. Like the ATA, it will consist of large numbers of individual elements and permit synthesis of multiple simultaneous beams. This joint project among the Naval Research Laboratory, The Netherlands Foundations for Research in Astronomy, and the Haystack Observatory, Massachusetts Institute of Technology is seeking design and development funding, and has a completion target date of about 2010.

For dedicated observations of the Sun, a frequency-agile solar array (FASR) is planned. This will consist of approximately 100 elements of 2–5-m diameter, covering a frequency range of 100 MHz–30 GHz. It will provide modest spectral resolution and short time resolution of about 0.1 s in order to observe fast-evolving solar phenomena such as flares. Completion is planned for approximately 2010.

Long-term planning by a huge international consortium is now in progress for the square kilometer array (SKA), which is intended to provide a collecting area of 1 km^2 at frequencies from 300 MHz to 22 GHz, with baselines up to 1000 km. The elements may consist of separate antennas for the lower and upper frequency regions. Like the ATA and LOFAR, the SKA is intended to provide synthesis of multiple simultaneous beams. This instrument would provide as great an increase over the VLA in sensitivity and resolution as the VLA provided over the single antennas and small interferometers of $\sim$1980. Much new

technology is required for practical construction of the SKA; in particular, the cost of collecting area must be reduced to approximately 10% of that of the ATA, which currently provides the most cost-effective antenna area of any radio telescope system. The completion date for this immense project is uncertain, but seems likely to fall between 2010–2020.

The most up-to-date information about all these projects is generally to be found on the Internet web sites of the organizations involved.

ACKNOWLEDGMENT

The authors thank A. Kerr for a critical review of this paper's manuscript. The National Radio Astronomy Observatory is a facility of the National Science Foundation operated under cooperative agreement by Associated Universities Inc.

REFERENCES

[1] K. G. Jansky, "Electrical disturbances apparently of extraterrestrial origin," *Proc. IRE*, vol. 21, p. 1387, Oct. 1933.
[2] J. D. Kraus, *Radio Astronomy*, 2nd ed. Powerll, OH: Cygnus Quasar Books, 1986.
[3] G. Reber, "Cosmic static," *Proc. IRE*, vol. 28, p. 68, Feb. 1940.
[4] P. F. Goldsmith, Ed., *Instrumentation and Techniques for Radio Astronomy*. New York: IEEE Press, 1988.
[5] H. Hirabayashi *et al.*, "Overview and initial results of the very long baseline interferometry space observatory program," *Science*, vol. 281, pp. 1825–1829, 1998.
[6] A. R. Thompson, J. M. Moran, and G. W. Swenson, Jr., *Interferometry and Synthesis in Radio Astronomy*, 2nd ed. New York: Wiley, 2001.
[7] T. A. Clark, B. E. Corey, J. L. Davis, G. Elgered, T. A. Herring, H. F. Hinteregger, C. A. Knight, J. I. Levine, G. Lundqvist, C. Ma, E. F. Nesman, R. B. Philips, A. E. E. Rogers, B. O. Ronnang, J. W. Ryan, B. R. Schupler, D. B. Shaffer, I. I. Shapiro, N. R. Vandenberg, J. C. Webber, and A. R. Whitney, "Precision Geodesy using the mark-III very-long-baseline interferometer system," *IEEE Trans. Geosci. Remote Sensing*, vol. GRE-23, pp. 438–449, July 1985.
[8] S. Okwit, "A historical view of the evolution of low-noise concepts and techniques," *IEEE Trans. Microwave Theory Tech.*, vol. MTT-32, pp. 1068–1082, Sept. 1984.
[9] J. J. Whelehan, "Low-noise millimeter-wave receivers," *IEEE Trans. Microwave Theory Tech.*, vol. MTT-25, pp. 268–280, Apr. 1977.
[10] S. Weinreb, "Low-noise, cooled GASFET amplifiers," *IEEE Trans. Microwave Theory Tech.*, vol. 28, pp. 1041–1054, Oct. 1980.
[11] S. Weinreb and A. Kerr, "Cryogenic cooling of mixers for millimeter and centimeter wavelength," *IEEE J. Solid-State Circuits*, vol. SSC-8, pp. 58–61, Feb. 1973.
[12] P. L. Richards *et al.*, "Quasiparticle heterodyne-mixing in SIS tunnel junctions," *Appl. Phys. Lett.*, vol. 34, no. 5, pp. 345–347, 1979.
[13] G. J. Dolan, T. G. Phillips, and D. P. Woody, "Low-noise 115 GHz mixing in superconducting oxide-barrier tunnel junctions," *Appl. Phys. Lett.*, pp. 347–349, 1979.
[14] J. R. Tucker, "Quantum-limited detection in tunnel junction mixers," *IEEE J. Quantum Electron.*, vol. QE-15, pp. 1234–1258, Nov. 1979.
[15] A. R. Kerr, S.-K. Pan, M. J. Feldman, and A. Davidson, "Infinite available gain in a 115 GHz SIS mixer," *Physica*, vol. 108B, pp. 1369–1370, 1981.
[16] J. Shell and D. Neff, "A 32 GHz reflected-wave maser amplifier with wide instantaneous bandwidth," in *Proc. IEEE MTT-S Int. Microwave Symp. Dig.*, New York, N.Y., June 1978, pp. 789–792.
[17] M. W. Pospieszalski, W. J. Lakatosh, R. Lai, K. L. Tan, D. C. Streit, P. H. Liu, R. M. Dia, and J. Velebir, "Millimeter-wave, cryogenically-coolable amplifiers using AlInAs/GaInAs/InP HEMT's," in *Proc. IEEE MTT-S Int. Microwave Symp. Dig.*, Atlanta, GA, June 1993, pp. 515–518.
[18] Y. L. Kok, H. Wang, T. Huang, R. Lai, M. Barsky, M. Sholley, T. Gaier, and L. Samoska, "160–190 GHz monolithic low-noise amplifiers," *Microwave Guided Wave Lett.*, vol. 9, pp. 314–316, Aug. 1999.
[19] R. Raja, M. Nishimoto, M. Barsky, M. Sholley, B. Osgood, R. Quon, G. Barber, P. Liu, P. Chin, R. Lai, and F. Hinte, "A 183 GHz low-noise amplifier module for the conical-scanning microwave imager sounder (CMIS) program," in *Proc. IEEE MTT-S Int. Microwave Symp. Dig.*, Boston, MA, June 11–16, 2000, pp. 987–999.
[20] S. Weinreb, R. Lai, N. Erickson, T. Gaier, and J. Wielgus, "W-band InP wideband MMIC LNA with 30 K noise temperature," in *Proc. IEEE MTT-S Int. Microwave Symp. Dig.*, Anaheim, CA, June 1999, pp. 101–104.
[21] M. W. Pospieszalski, W. J. Lakatosh, E. J. Wollack, L. D. Nguyen, M. Le, M. Lui, and T. Liu, "Millimeter-wave waveguide-bandwidth cryogenically-coolable InP HEMT amplifiers," in *Proc. IEEE MTT-S Int. Microwave Symp. Dig.*, Denver, CO, June 1997, pp. 1285–1288.
[22] M. W. Pospieszalski, "Cryogenically-cooled, HFET amplifiers and receivers: State-of-the-art and future trends," in *Proc. IEEE MTT-S Int. Microwave Symp. Dig.*, Albuquerque, NM, 1992, pp. 1369–1372.
[23] J. R. Tucker and M. J. Feldman, "Quantum detection at millimeter wavelengths," *Rev. Mod. Phys.*, vol. 57, no. 4, pp. 1055–1113, 1985.
[24] S. Padin, D. P. Woody, J. A. Stern, H. G. LeDuc, R. Blundell, C.-Y. E. Tong, and M. W. Pospieszalski, "An integrated SIS mixer and HEMT IF amplifier," *IEEE Trans. Microwave Theory Tech.*, vol. 44, pp. 987–990, June 1996.
[25] E. F. Lauria, A. R. Kerr, M. W. Pospieszalski, S.-K. Pan, J. E. Effland, and A. W. Lichtenberger, "A 200–300 GHz SIS mixer–preamplifier with 8 GHz IF bandwidth," in *IEEE MTT-S Int. Microwave Symp. Dig.*, vol. 3, 2001, pp. 1645–1648.
[26] A. R. Kerr, S.-K. Pan, A. W. Lichtenberger, and H. H. Huang, "A tunerless SIS mixer for 200–280 GHz with low output capacitance," presented at the 9th Int. Space Terahertz Technol. Symp., 1998.
[27] A. R. Kerr, S.-K. Pan, and H. G. LeDuc, "An integrated sideband separating SIS mixer for 200–280 GHz," presented at the 9th Int. Space Terahertz Technol. Symp., 1998.
[28] J. C. Webber, A. R. Kerr, S.-K. Pan, and M. W. Pospieszalski, "Receivers for the millimeter array," in *Proc. SPIE Advanced Technol. MMW, Radio, Terahertz Telescopes Conf.*, 1998, pp. 122–131.
[29] S. Weinreb, M. W. Pospieszalski, and R. Norrod, "Cryogenic, HFET, low noise receivers for 1.3 to 43 GHz range," in *Proc. IEEE MTT-S Int. Microwave Symp. Dig.*, New York, N.Y., June 1988, pp. 945–948.
[30] P. J. Napier, "The large synthesis radio telescope of the national radio astronomy observatory," in *Proc. IEEE MTT-S Int. Microwave Symp. Dig.*, Albuquerque, NM, June 1992, pp. 1243–1246.
[31] R. D. Norrod, S. Srikanth, and M. Balister, "The receiver and optics designs for 100-meter Green Bank telescope," in *Proc. IEEE MTT-S Int. Microwave Symp. Dig.*, Albuquerque, NM, June 1992, pp. 1365–1368.
[32] M. W. Pospieszalski, E. J. Wollack, N. Bailey, D. L. Thacker, J. C. Webber, L. D. Nguyen, M. Le, and M. Lui, "Design and performance of wideband, low-noise, millimeter-wave amplifiers for microwave anisotropy probe radiometers," in *Proc. IEEE MTT-S Int. Microwave Symp. Dig.*, Boston, MA, June 11–16, 2000, pp. 25–28.
[33] C. Bennett, G. Hinshaw, N. Jarosik, J. C. Mather, S. S. Meyer, L. Page, D. N. Spergel, D. T. Wilkinson, and E. L. Wright, "Microwave anisotropy probe (MAP) MIDEX proposal," NASA Goddard Space Flight Center, Greenbelt, MD, Dec. 1995.
[34] N. Jarosik, "The use of cryogenic HEMT amplifiers in wide band radiometers," presented at the GAAS Conf., Paris, France, Oct. 2, 2000.
[35] J. M. Moran, "The submillimeter array," in *Proc. SPIE Advanced Technol. MMW, Radio, Terahertz Telescopes Conf.*, 1998, pp. 208–219.
[36] R. L. Brown, "Technical specification of the millimeter array," in *Proc. SPIE Advanced Technol. MMW, Radio, Terahertz Telescopes Conf.*, 1998, pp. 231–237.
[37] S. Guilloteau, "LSA project," in *Proc. SPIE Advanced Technol. MMW, Radio, Terahertz Telescopes Conf.*, 1998, pp. 238–243.
[38] M. Ishiguro, "Japanese large millimeter and submillimeter array," in *Proc. SPIE Advanced Technol. MMW, Radio, Terahertz Telescopes Conf.*, 1998, pp. 244–253.
[39] R. Blundell, C.-Y. E. Tong, D. C. Papa, R. L. Leombruno, X. Zhang, S. Paine, J. Stern, H. G. LeDuc, and B. Bumble, "A wideband fixed-tuned SIS receiver for 200 GHz operation," *IEEE Trans. Microwave Theory Tech.*, vol. 43, pp. 933–937, Apr. 1995.
[40] C.-Y. E. Tong, R. Blundell, S. Paine, D. C. Papa, J. Kawamura, J. Stern, and H. G. LeDuc, "Design and characterization of a 250–350 GHz fixed-tuned superconductor–insulator–superconductor receiver," *IEEE Trans. Microwave Theory Tech.*, vol. 44, pp. 1548–1556, Sept. 1996.
[41] A. R. Kerr, S.-K. Pan, A. W. Lichtenberger, N. Horner, J. E. Effland, and K. Crady, "A single-chip balanced SIS mixer for 200–300 GHz," in *Proc. 11th Int. Space Terahertz Technol. Symp.*, Ann Arbor, MI, May 2000, pp. 251–259.

[42] A. R. Kerr and S.-K. Pan, "Design of planar image-separating and balanced SIS mixers," in *Proc. 7th Int. Space Terahertz Technol. Symp.*, Mar. 1996, pp. 207–219.
[43] A. R. Kerr, "Suggestions for revised definitions of noise quantities, including quantum effects," *IEEE Trans. Microwave Theory Tech.*, vol. 47, pp. 325–329, Mar. 1999.
[44] S.-K. Pan, A. R. Kerr, M. J. Feldman, A. W. Kleinsasser, J. Stasiak, R. L. Sandstrom, and W. J. Gallagher, "An SIS mixer for 85–116 GHz using inductively shunted edge-junctions," in *IEEE MTT-S Int. Microwave Symp. Dig.*, 1988, pp. 465–468.

John C. Webber received the B.S. and Ph.D. degrees in astronomy from the California Institute of Technology, Pasadena, in 1964 and 1969, respectively.

From 1970 to 1980, he was an Assistant Professor in the Astronomy and Electrical Engineering Departments, University of Illinois at Urbana-Champaign, where he conducted research in radio astronomy and developed instrumentation for a 120-ft-diameter radio telescope. From 1980 to 1988, he was Assistant Director of Haystack Observatory, Massachusetts Institute of Technology (MIT), Westford, where he developed instrumentation for VLBI. From 1988 to 1996, he was Vice President of Interferometrics Inc., Vienna, VA, where he produced radio astronomy data acquisition equipment. He also patented and put into practice commercial applications of radio interferometry, including a method of locating transmitters, which interfere with geosynchronous satellite communications, and a method of locating cellular telephones. Since 1996, he has been Assistant Director of the National Radio Astronomy Observatory (NRAO), Charlottesville, VA, and Director of the NRAO Central Development Laboratory. His research interests are in all areas of radio astronomy instrumentation, with emphasis on the EVLA, ALMA, and GBT.

Dr. Webber is a member of the American Astronomical Society, the International Astronomical Union, and URSI Commission J.

Marian W. Pospieszalski (M'85–SM'85–F'92) received the M.Sc. and D.Sc. degrees in electronic engineering from the Warsaw University of Technology, Warsaw, Poland, in 1967 and 1976, respectively.

From 1967 to 1984, he was with the Institute of Electronics Fundamentals, Warsaw University of Technology, during which time he held visiting positions with the Electronics Research Laboratory, University of California at Berkeley (1977–1978) and the National Radio Astronomy Observatory (NRAO), Charlottesville, VA (1978–1979), and the Department of Electrical Engineering, University of Virginia, Charlottesville (1982–1984). From 1984 to 2001, he was with the NRAO, where he was involved with the theory and design of low-noise devices, amplifiers, and receivers for radio astronomy applications. In 2001, he became Chief Scientist, Microwave at Inphi Corporation, Westlake Village, CA, a company that develops high-speed circuits for optical communications. His research interests are in the field of microwave, millimeter-wave, and high-speed circuits and systems.

Dr. Pospieszalski is a member of URSI Commissions D and J.